Development of Levitation Experiments for Teaching Purposes

Hugo P. Ferreira, Alan Dantas de M. Endalécio and Richard M. Stephan
Universidade Federal do Rio de Janeiro, Rio de Janeiro, Brazil
hugopelle@poli.ufrj.br,
alanendalecio@poli.ufrj.br,richard@dee.ufrj.br

Abstract

The objective of this paper is to present two magnetic levitation experiments, which give a first didactic approach to the concepts necessary to understand magnetic bearings.

On the first experiment, an electrodynamic levitation system with alternating current, capable of levitating metallic rings will be presented.

On the second experiment, an electromagnetic levitation system, using a Hall effect sensor to measure the levitated object position – a ferromagnetic sphere combined with permanent magnets – will be described.

These laboratory rigs demonstrate the importance of simulation tools and experimental work on the verification of theoretical concepts learned in Electrical/Electronic Engineering classes.

1 Introduction

The development of levitation systems allows engineering students to better understand the concepts of Electromagnetism, Control Systems, Microelectronics, Power Electronics, Instrumentation and Numerical Analysis, besides allowing a first contact with the magnetic bearings area.

The Laboratory of Applied Superconductivity (LASUP) developed a wide range of experiments based on three main levitation techniques: superconducting levitation (SML), electromagnetic levitation (EML) and electrodynamic levitation (EDL) [1-5]. These experiments have teaching purposes and combine simulation, theory, numerical analysis tools and experimental results.

This work presents the development of two of these magnetic levitation experiments, the first one using the electrodynamic technique and the second one using the electromagnetic levitation technique.

2 Electrodynamic Levitation System

The electrodynamic levitation is based on Faraday's Law that states that a time variant magnetic field on the neighborhood of a conductor material will induce an electromotive force that, on the other hand, will develop an electric current on the conductor. This current circulates on such a way that, by Lenz's law, a magnetic field is established with the objective to cancel the magnetic flux variation on the material.

Electrodynamic levitation experiments with teaching purposes are fairly widespread in the literature [6] and a lot of them have in common the supply of alternate currents on coils and turns.

This experiment is based on reference [7] and consists on achieving magnetic levitation of conductor rings from the application of alternate voltage to a coil. The alternate magnetic field produces an electromotive force on the ring responsible to generate an alternate current that establishes a magnetic field that opposes to the first. The objective of this experiment is to obtain levitation of two metallic rings, the first one of aluminum and the other of copper, using the electric grid voltage of 127 V rms.

2.1 Methodology

With the coil and the rings, that can be seen in Fig. 1, a preliminary test with the objective to verify the system behavior was performed. On this test, a sinusoidal voltage of variable amplitude, maintaining the frequency of 60 Hz, was applied until the levitation of each ring. The result shows that the levitation of the aluminum ring and the copper ring begins when a 250 V rms voltage and a 450 V rms are applied to the coil, respectively. When the applied voltage was 450 V rms, the stable levitation height of aluminum ring and copper ring was 9.9 cm and 6.0 cm, respectively.

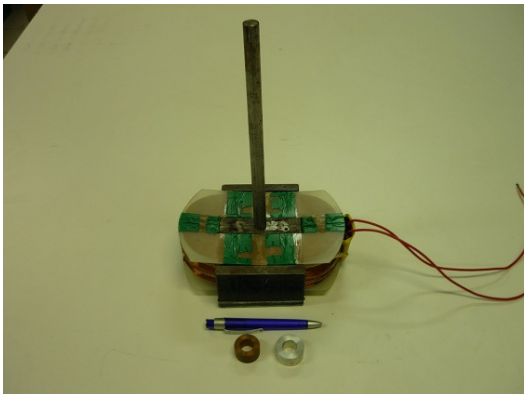

Figure 1: Electrodynamic levitation system and metallic rings: copper (left) and aluminum (right).

The next step was the development of a reliable computational model that could be able to represent properly the electrodynamic system. This could be done with the finite element analysis package COMSOL Multiphysics. The software has an AC/DC simulation module that can perform analysis of electromagnetic systems in 1D, 2D and 3D. The electrodynamic system has axial symmetry, so a 2D Axis-symmetric model was developed on the software. Figure 2 presents the simulation package interface together with a finite element mesh of the simulated system.

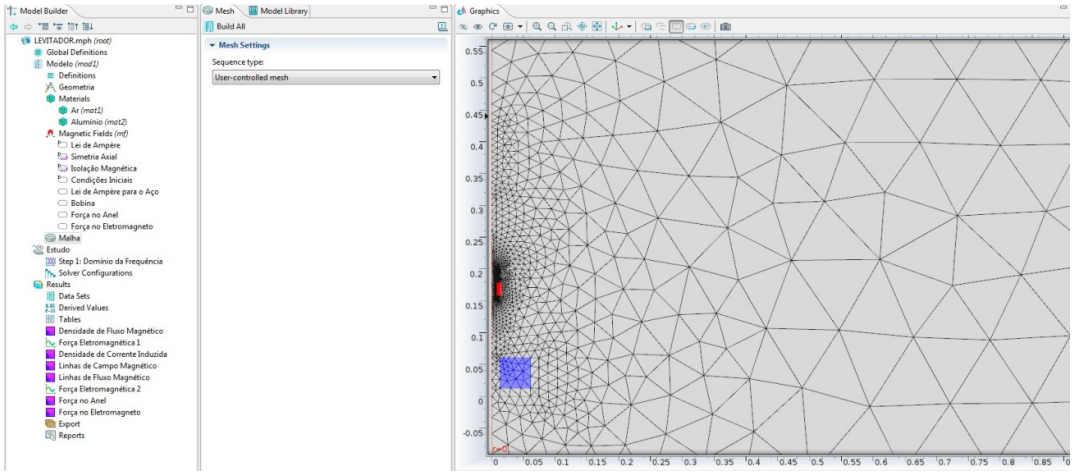

Figure 2: Finite element mesh generated by COMSOL Multiphysics and its interface.

The simulations were performed on the following way: every ring was positioned on different heights and the result was the corresponding levitation force. The coil was supplied by a sinusoidal voltage of 450 V rms and a frequency of 60 Hz. The simulation results are presented in Fig. 3 for the aluminum ring and the copper ring compared with the experimental results.

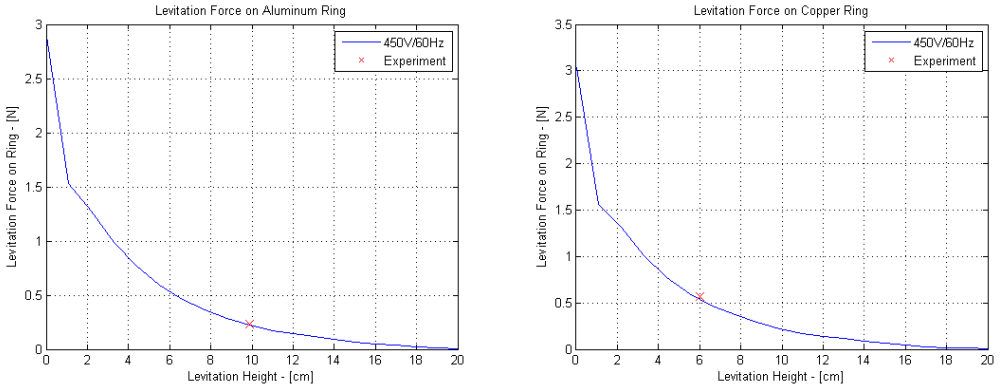

Figure 3: Simulation results for the aluminum ring (left) and the copper ring (right) compared with experimental results.

The results presented in Fig. 3 demonstrate that the computational model was correct since, on the stable levitation height of each ring, the simulation and the experimental results are very close. With a reliable model, it was possible to make simulations with the desirable configuration.

To achieve this objective, two kinds of simulations were developed, with a voltage of 127 V rms applied to the coil. The first kind performed simulations changing the parameters of the coil and the ring, like number of turns, cross section of the wire and dimensions of the ring. The second kind performed simulations changing the frequency of the sinusoidal voltage.

This second one indicated that the frequency needed to be reduced from 60 Hz to 15 Hz. Figure 4 presents the simulation results of the second solution for the aluminum and copper rings that represent a new configuration of the system compared with the simulation results of Fig. 3 (original configuration).

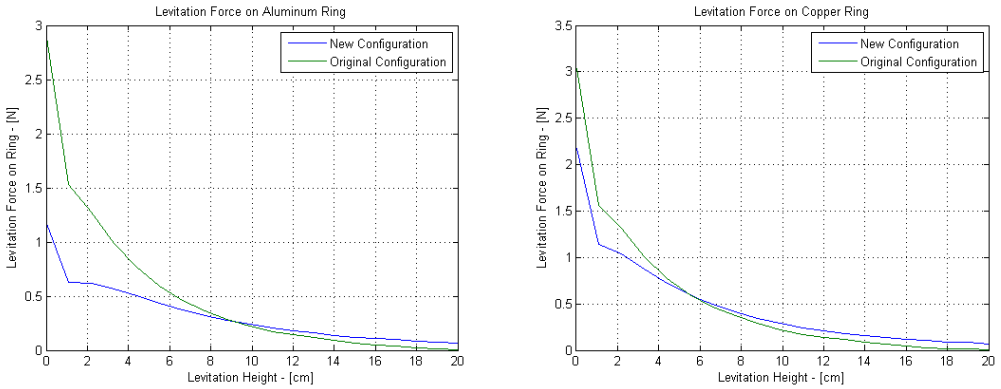

Figure 4: Simulation results of the new configuration (127 V/15 Hz) compared with simulation results of the original configuration (450 V/60 Hz) for aluminum (left) and copper (right) ring.

The simulation results show that the curves obtained for the original and new configurations intersect at the position of stable equilibrium of both rings. However, it was expected that the curves were superimposed over the entire range of levitation heights, since the ratio voltage (V) to frequency (f) remained approximately constant. The reason for this difference lies in the fact that the electromagnet comprises an inductive portion associated with a resistive part that is not negligible at low frequencies, like 15 Hz. Therefore, the levitation force does not have a direct relation with the ratio V/f at all levitation heights. The frequency change was realized using one phase of a 3 phase frequency inverter.

3 Electromagnetic Levitation System

Due to its interdisciplinary characteristic (involving subjects of control, electromagnetic theory, electronics, analogical and digital circuits, etc…), magnetic suspension experiments have a strong didactic appeal for engineering courses.

The Laboratory of Applied Superconductivity (LASUP) has developed this kind of experiments over the years [8-11], but the high implementation cost became a great obstacle for didactic application, mainly because the high price of position sensors.

This work presents a low-cost suspension system using a Hall Effect sensor (SS495A) [12-14], replacing the traditional position sensors, which are used in electromagnetic suspension systems. Electrical sensors, as the one used in this project, are cheaper and smaller than mechanic sensors.

The Hall Effect sensor measures the magnetic flux density, therefore it was necessary to fasten permanent magnets of Nd-Fe-B to the levitated object.

As it will be presented throughout the study, this suspension system is naturally unstable. That's why a negative feedback loop with a controller is included, to stabilize the system.

In this work, a digital control with *Arduino* will be used. *Arduino* is a low-cost developing environment that uses a micro controller (ATMEGA328P). The developing language is very easy, also for beginners. An application of micro controller in this kind of project can be found in [15].

3.1 System operation

The system diagram can be seen in Fig. 5.

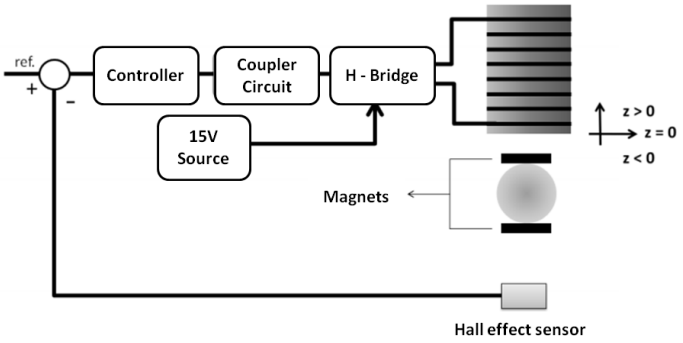

Figure 5: Electromagnetic suspension system diagram.

The system works following the logic:

1) Hall Effect sensor measures the suspended object position and sends a voltage signal to the micro controller. The SS495A Hall effect sensor, with an output voltage ranging between 0 and 5 Volts was used.
2) The control system processes this signal, compares it with a reference value and generates a PWM control signal that is sent to the coupler circuit. This circuit is responsible to isolate the micro controller from the power electronics circuits, for safety reasons, providing an output signal that is identical to its input signal.
3) The coupler circuit output signal is sent to a H-bridge, which switches the voltage on the electromagnet between , according to PWM control, controlling the average level of voltage on the electromagnet. It was adopted the LMD18201, an integrated H bridge.
4) Controlling the average level of voltage, it's possible to change the average value of circulating current, controlling the magnetic field, produced by this current, and thus to keep the desired gap between electromagnetic coil and object.

3.2 Dynamic of the system

In electromagnetic suspension, it's known that the force produced by an electromagnet is proportional to the square of current and inversely proportional to the square of distance (gap). However, the presence of magnets changes the relationship among magnetic force, current and distance.

According [16], the magnetic flux density produced by an electromagnet can be expressed as:

$$B(i,z) = \frac{\mu_0 i N R^2}{2(R^2 + z^2)^{3/2}} \tag{1}$$

where,

B is the magnetic flux density produced by the electromagnet;
μ_0 is the magnetic permeability of air;
N is the number of turns;
R is the radius of electromagnet;
z is the distance where the magnetic field is measured from electromagnet.

The produced magnetic force above a magnet by an external magnetic field may be expressed as [17]:

$$F_M = \vec{n} \, . \, \frac{d\vec{B}}{dz} \tag{2}$$

where,

F_M is the magnetic force;
$\vec{n}$ is the magnetic moment of the magnet.

Replacing the first equation on second one, the following results:

$$F_M(z,i) = -K \frac{i \, z}{(R^2 + z^2)^{\frac{5}{2}}} \tag{3}$$

with $K = \frac{3}{2} N n \mu_0 R^2$.

The system dynamics may be expressed by Newton's second law as:

$$m\ddot{z} = F_M - mg \tag{4}$$

The system can be linearized around an equilibrium point (i_0, z_0), as demonstrated by Eq. (5):

$$m\ddot{\Delta z} = K_i \Delta i + K_z \Delta z \tag{5}$$

with

$$K_i = \frac{-K z_0}{(R^2 + z^2)^{5/2}} \text{ and } K_z = -K i_0 \left(\frac{R^2 - 4{z_0}^2}{(R^2 + z^2)^{7/2}} \right).$$

Applying Laplace's transform to equation (5), the system transfer function is represented by Eq (6):

$$H(s) = \frac{\Delta Z(s)}{\Delta I(s)} = \frac{K_i/m}{s^2 - K_z/m} \tag{6}$$

As the system control is realized by the voltage applied to the solenoid, it's possible to rewrite Eq. (6), knowing that $\Delta I(s) = \Delta V(s)/(R_L + Ls)$, being R_L and L the resistance and inductance of the solenoid, respectively.

$$H(s) = \frac{\Delta Z(s)}{\Delta V(s)} = \frac{K_i/m}{\left(s^2 - \frac{K_z}{m}\right)(R_L + Ls)} \tag{7}$$

Table 1 shows the values of equation 7 for the laboratory system.

Table 1: Transfer function parameter values.

Parameter	Description	Value
m (g)	Mass of levitated object	17.0
z_0 (mm)	Equilibrium position	-11.0
i_0 (mA)	Equilibrium current	147.0
K_i (N/A)	Linearization constant	1.1
K_z (N/m)	Linearization constant	33.9
R_L (Ω)	Solenoid resistance	6.1
L (mH)	Solenoid inductance	38.3

Replacing the parameters for their values, the transfer function is expressed by Eq. (8):

$$H(s) = \frac{\Delta Z(s)}{\Delta V(s)} = \frac{1742.3}{(s^2 - 1996)(s + 158.8)} \tag{8}$$

3.3 Lead controller design

The system becomes unstable by the presence of the positive pole on the transfer function. To change this, a Lead controller was projected, as expressed in Eq. (9):

$$C(s) = K\frac{(s + 45)}{(s + 800)} \tag{9}$$

In Figure 6, the compensated system root locus is shown.

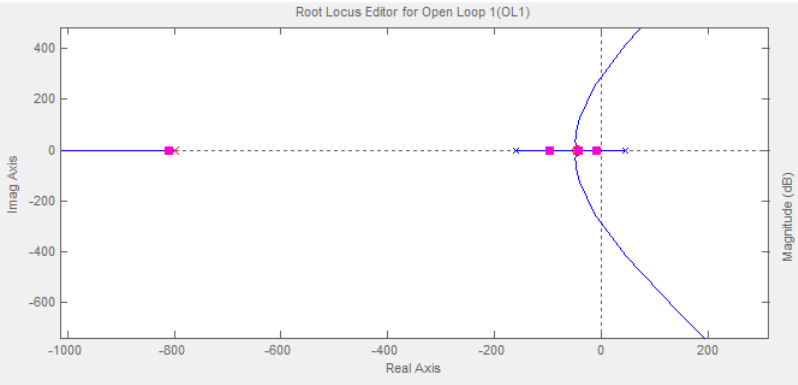

Figure 6: Compensated system root locus.

The gain K was determined experimentally to obtain a stable system. In this work, a digital Lead controller was used, obtained by equation (9) using the backward approximation, as expressed by equation (10).

$$u(n) = \frac{1}{(1 + 800T_s)}u(n-1) + \frac{K(1 + 45T_s)}{(1 + 800T_s)}e(n) - \frac{K}{(1 + 800T_s)}e(n-1) \tag{10}$$

where,

$u(n)$ is the control signal;
$e(n)$ is the feedback error signal;
T_s is the sampling period.

In this project, the ADC conversion frequency was increased to decrease the sampling period and an internal interruption was used to keep the sampling time always with the same value. In Figures 7 and 8, the control code of the system is shown.

```
//Lead Controller

// define global variable                                                    Block 1
int z = 45; //controller's zero
int p = 800; //controller's polo
double T = 0.000212; //Sampling period in seconds
double vsensor; //Hall effect sensor output
double K = (800/45); //Lead controller gain
double u; //control signal
double ref = 0.6; //reference
double erro; //feedback error
double erro_ant = 0; //previous feedback error
double u_ant = 0; //previous control signal

// Lead controller constants
double K1 = K*(1 + (z*T))/(1 + (p*T));
double K2 = -K/(1 + (p*T));
double K3 = 1/(1 + (p*T));

// Define ADC prescalers                                                     Block 2
const unsigned char PS_64 = (1 << ADPS2) | (1 << ADPS1);
const unsigned char PS_128 = (1 << ADPS2) | (1 << ADPS1) | (1 << ADPS0);

void setup(){
  cli(); //stop interruption

  //Change ADC frequency
    // set up the ADC
    ADCSRA &= ~PS_128;  // removing previous configurated bits by Arduino

    ADCSRA |= PS_64;    // ADC prescaler as 64

  //Adjusting sampling period to 212us                                        Block 3
  TCCR1A = 0;
  TCCR1B = 0;
  TCNT1 = 0;
  // "compare match register" for period of 212us
  OCR1A = 423; // = (16*10^6)/(8*(1/212u)) - 1 (must be < 65536)
  // CTC mode enable
  TCCR1B |= (1 << WGM12);
  // timer prescaler as 8
  TCCR1B |= (1 << CS11);
  //interruption call enable
  TIMSK1 |= (1 << OCIE1A);

  sei(); //allow interruption
}
```

Figure 7: Control code.

The control code has three main blocks. The first block is responsible to define the global variables that are used. The second block shows the code part responsible to increase the ADC frequency and, therefore, reduce the total sampling period [18]. The third block is responsible to configure one of Arduino's counters to call an interruption every sampling period [19]. A sampling period of 212 µs and a Lead controller gain of 17.8 were used.

```
ISR(TIMER1_COMPA_vect){

  vsensor = analogRead(0); //Reading Hall effect sensor output
  vsensor = 5*vsensor/1023; // Convert for a range between 0 and 5
  erro = -ref + vsensor; // Feedback error calculation
  u = K1*erro + K2*erro_ant + K3*u_ant; // Lead controller
  analogWrite(11,(250*u/5)); //PWM signal generation
  u_ant = u;
  erro_ant = erro;
}

void loop(){

}
```

Figure 8: Lead controller code.

Figure 8 presents the developed Lead controller for this project. Initially, it reads the Hall Effect sensor output, using the *analogRead* function and convert for a range between 0 and 5 vots. After that, the feedback error and the control signal using the expression showed in Eq. (10) are calculated. In the following, the PWM signal is generated and the values of *u_ant* and *erro_ant* variables are realized.

4 Results

When the coil of the electrodynamic system was supplied by a sinusoidal voltage of 127 V rms and 15 Hz, the values presented by computational simulation were verified. Figure 9 shows the levitation of both rings performed on this test.

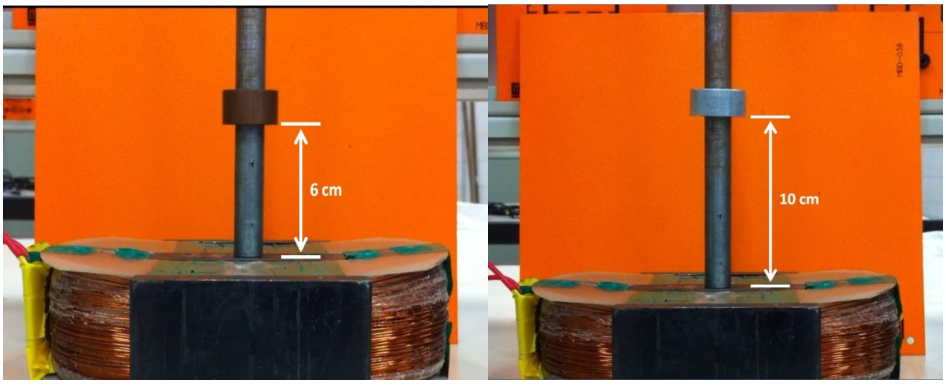

Figure 9: Levitation of the copper (left) and aluminum (right) ring using 15 Hz and 127 V.

The electromagnetic system presented good results for a constant reference. The main controller goals were: to stabilize the system and to be able to change the gap, changing the reference and keeping stability. So the reference was changed, increasing or decreasing the original value, to evaluate the system response. As expected, it was possible to observe an increasing or decreasing gap when the reference value changed. A picture of the electromagnetic system can be seen in Figure 10.

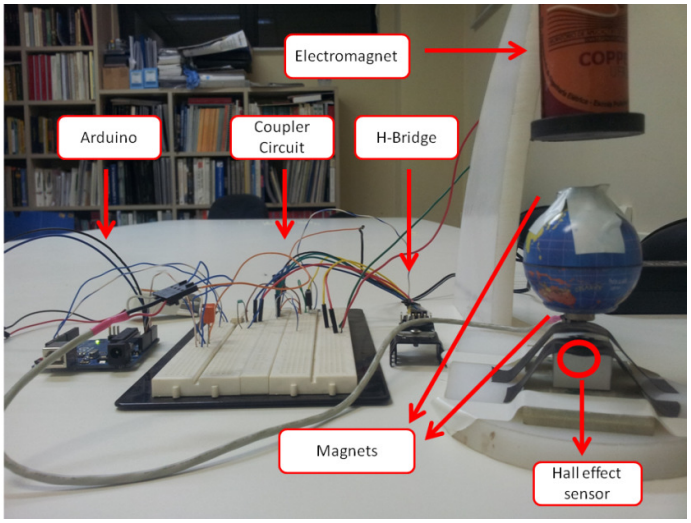

Figure 10: Electromagnetic suspension system.

5 Conclusion

The main objective of this work was to present laboratory experiments of magnetic levitation that could be used for teaching purposes. To perform these experiments, several subjects explored on engineering courses were addressed, for instance: mathematical modeling of physical systems, simulations, numerical analysis, programming and design of control systems using microcontrollers.

According to the results presented in this work, these experiments could be seen as motivation to undergraduates to study magnetic bearings.

6 Acknowledgement

To CNPq and FAPERJ for the financial support.

7 References

[1] Valle, R. L. S.; Neves, F. F.; De Andrade, R. and Stephan, R. M.: Electromagnetic Levitation of a Disc, *IEEE Transactions on Education*, Vol. 55, 2012, p. 248-254.

[2] Sotelo, G. G.; Stephan, R. M.; Branco, P. J. C. and De Andrade, R.: A Didactic Comparison of Magnetic Forces, *International Journal of Electrical Engineering Education*, Vol. 48, 2011, p. 117-129.

[3] Gomes, R. R.; Sotelo, G. G. and Stephan, R. M.: Comparação de Configurações para um Levitador Eletromagnético pelo Método dos Elementos Finitos, 6th Congresso Brasileiro de Eletromagnetismo, 2004, São Paulo.

[4] Gomes, R. R.; Sotelo, G. G. and Stephan, R. M.: Desenvolvimento de um Sistema Didático para Levitação Eletromagnético com o Auxílio do Método dos Elementos Finitos, XV Congresso Brasileiro de Automática, 2004, Gramado.

[5] Stephan, R. M.; Machado, O. J.; Forain, I. and De Andrade, R.: Experiências de Levitação Magnética, XIII Congresso Brasileiro de Automática, Vol. 1, 2002, Natal, p. 309-312.

[6] Laithwaite, E. R.: Electromagnetic Levitation, *Proceedings of Institution of Electrical Engineers*, Vol. 112, Issue 12, Dec. 1965, pp. 2361-2375.

[7] Jayawant, B. V.: Electromagnetic Suspension and Levitation, *IEE Proceedings A*, Vol. 129, Issue 8, Nov. 1982, pp. 549-581.

[8] Gomes, R. R.: Um Experimento para Ilustrar o Sistema de Levitação Eletromagnética Utilizado em Trens Maglev, UFRJ, Rio de Janeiro, 2004.

[9] Mota, D. J. P. S.: Controle da Posição de uma Esfera em um Sistema de Levitação Eletromagnética, Dept. Elect. Eng., UFRJ, Rio de Janeiro, Brazil, B. Sc. Rep., 2008.

[10] Neves, F. F.: Controle Adaptativo Programado, Rejeição de Distúrbios e Estimador de Posição Aplicado ao Sistema de Levitação Eletromagnética de um Disco, Dept. Automation and Control, UFRJ, Rio de Janeiro, Brazil, B. Sc. Rep., 2012.

[11] Valle, R. L. S.: Levitação Eletromagnética de um Disco, Dept. Elect. Eng., UFRJ, Rio de Janeiro, Brazil, B. Sc. Rep., 2010.

[12] Lilienkamp, K. A. and Lundberg, K.: Low-cost magnetic levitation project kits for teaching feedback system design, American Control Conference, Proceedings of the 2004, Vol. 2, p. 1308-1313.

[13] http://www.arttec.net/Levitation (Access in August 12th, 2013).

[14] http://www.arttec.net/Levitation/Gallery/Levitator.PDF (Access in August 14th, 2013).

[15] Artigas, J. I.; Barragán, L. A.; Llorente, S.; Marco, A. and Lucía, O.: Low-Cost Magnetic Levitation System for Electronics Learning, 4th IEEE International Conference on E-Learning in Industrial Electronics, Nov. 2010, p. 55-60.

[16] Halliday, D. and Resnick, R. W.: *Fundamentos de Física – Eletromagnetismo*, 6th ed., v.3, Ed. LTC, 2001.

[17] Purcell, E.M.: *Curso de Física de Berkeley, Volume 2 – Eletricidade e Magnetismo*, São Paulo, Ed. Edgar Blucher Ltda., 1965.

[18] http://www.marulaberry.co.za/index.php/tutorials/code/arduino-adc/ (Access in August 10th, 2013).

[19] http://www.instructables.com/id/Arduino-Timer-Interrupts/ (Access in August 10th, 2013).